

## Article

# Gelatin–Siloxane Hybrid Monoliths as Novel Heavy Metal Adsorbents

Patrycja Wojciechowska <sup>1</sup>, Ryszard Cierpiszewski <sup>1,\*</sup> and Hieronim Maciejewski <sup>2,3</sup>

<sup>1</sup> Department of Industrial Products and Packaging Quality, Poznan University of Economics and Business, 61-875 Poznan, Poland; patrycja.wojciechowska@ue.poznan.pl

<sup>2</sup> Faculty of Chemistry, Adam Mickiewicz University, 61-614 Poznan, Poland; maciejm@amu.edu.pl

<sup>3</sup> UAM Foundation, Poznan Science and Technology Park, 61-612 Poznan, Poland

\* Correspondence: ryszard.cierpiszewski@ue.poznan.pl; Tel.: +48-61-8569-027

**Abstract:** Novel gelatin-siloxane hybrid monoliths for heavy metal removal were prepared in the chemical reaction of gelatin with organomodified silicone containing epoxy group. Obtained porous hybrid materials were applied for adsorption of Cu(II), Cd(II) and Pb(II) from aqueous solutions. In this paper, the influence of siloxane amount used for the modification of gelatin on adsorbent stability and heavy metal removal was examined. The effect of pH values of the immersion liquid, as well as the contact time, was studied. Morphology, compressive strength and water absorption of hybrid monoliths were investigated. Desorption tests were also performed. The results showed that the higher the amount of the siloxane, the better stability of the hybrid monoliths in aqueous solutions. The highest values of adsorption capacity were observed for Pb(II) ions. The experimental maximum adsorption capacity determined for hybrid monoliths was 3.75 mg/g for Pb(II), 1.76 mg/g for Cu(II) and 1.5 mg/g for Cd(II). The desorption of metal ions for hybrid monoliths stable in aqueous solutions reached 70%.



**Citation:** Wojciechowska, P.; Cierpiszewski, R.; Maciejewski, H. Gelatin–Siloxane Hybrid Monoliths as Novel Heavy Metal Adsorbents.

*Appl. Sci.* **2022**, *12*, 1258.

<https://doi.org/10.3390/app12031258>

app12031258

Academic Editors: Satoshi Komasa, Yoshiro Tahara, Tohru Sekino and Joji Okazaki

Received: 30 December 2021

Accepted: 22 January 2022

Published: 25 January 2022

**Publisher's Note:** MDPI stays neutral with regard to jurisdictional claims in published maps and institutional affiliations.



**Copyright:** © 2022 by the authors. Licensee MDPI, Basel, Switzerland. This article is an open access article distributed under the terms and conditions of the Creative Commons Attribution (CC BY) license (<https://creativecommons.org/licenses/by/4.0/>).

**Keywords:** gelatin; siloxane; heavy metal; adsorption; copper; cadmium; lead

## 1. Introduction

Heavy metal pollution has become a globally recognized environmental issue due to the extensive anthropogenic activities connected with rapid industrialization [1–3]. The main sources of heavy metal release into environment are wastewaters from chemical industries such as metal plating facilities, mining operations, battery manufacturing, fertilizer, paper or metallurgical industries, pesticides and tanneries [4]. Heavy metal ions such as lead, chromium, cadmium, arsenic, mercury, nickel, zinc and copper are hazardous above certain ppm concentration and toxic for human health. These contaminants do not biodegrade, show high solubility in the aquatic environments and tend to accumulate into body of living organisms. They have already been found in the food chains of aquatic species [1,4,5]. Long-term exposure to heavy metals causes defects to organs (e.g., kidney, lungs, liver, eyes) and biological entities such as the nervous system, immune system, reproductive system and respiratory system. It may contribute to several degenerative diseases of central nervous system, as well as damage of cardiovascular and gastrointestinal systems. Heavy metals increase the risk of anaemia, cancer, nausea, organ failure, loss in bone mineral, and tumour induction [1,2,6,7]. Research has shown that copper, nickel, lead, and arsenic have been observed to be toxic even at low concentrations [4], therefore effective methods of their removal from ecosystem are of importance. In the light of the above, the World Health Organization (WHO) established guidelines for drinking-water quality and recommended maximum permissible limits for selected heavy metals. Similar standards for drinking water have been developed also by the United States Environmental Protection Agency (USEPA) and the European Union (EU) [4].

Recently, different attempts have been made to solve the problem of effective heavy metal ions removal from wastewater. These methods include chemical precipitation, ion-exchange, adsorption, membrane filtration, coagulation–flocculation, bioremediation, flotation and electrochemical methods [1,2,5]. Among them adsorption has gained in importance as an effective way to treat industrial waste effluents, offering several advantages like low-cost, availability, profitability, and ease of operation. It serves as an alternative to conventional methods such as precipitation or coagulation. [2,3]. Moreover, while adsorption is sometimes reversible, once employed adsorbent can be regenerated by a suitable desorption process [2,4]. In principle, adsorption is a mass transfer process by which a substance is transferred from the liquid phase to the surface of a solid, and becomes bound by physical and/or chemical interactions [5]. A number of materials have been reported as adsorbents such as activated carbon, carbon nanotubes, chitosan, gelatin, zeolites, clay, or waste products from industrial operations i.e., fly ash, coal, and oxides. The use of natural materials for heavy metal removal offers some advantages as they are inexpensive and locally available [1,8].

To a large extent, the adsorption ability of various materials can be attributed to their morphology. The effectiveness of the removal of heavy metals is dependent on the surface area and adsorption capacity [5]. Thus, fabrication of highly porous structures, also using natural biopolymers is an interesting approach for the preparation of novel adsorbents. An interesting and wide group of heavy metal porous adsorbents that can be applied for water purification are aerogels. Depending on the chemical composition (organic, inorganic or both), and the synthetic route applied for the preparation, such materials exhibit tuneable morphology and efficiency [9]. Other examples of effective adsorbents are described by Li et al. [10] who developed highly porous inorganic materials derived from metal-organic frameworks suitable for Hg(II) elimination from aqueous solutions. Among new possible routes for preparation of new materials exhibiting high removal efficiency and adsorption capacity, synthesis of organic-inorganic hybrids can be taken into consideration.

Organic–inorganic hybrids represent a group of materials that combine the advantages of organic polymer (such as elasticity, formability, toughness) and inorganic compound (like hardness, strength, high chemical resistance and thermal stability) [11,12]. According to the definition provided by IUPAC (International Union of Pure and Applied Chemistry): “A hybrid material is composed of an intimate mixture of inorganic components, organic components, or both types of components. The components usually interpenetrate on a scale of less than 1  $\mu\text{m}$ ” [13]. It is worth noting that hybrid materials represent a synergetic combination of inorganic and organic components and they are not just simple physical mixtures of their constituents. Thus, properties they reveal are not the sum of the individual contributions of both phases but are dependent on the inner interfaces between them. Depending on the nature of the interface, hybrid materials are divided into two classes: *class I* and *class II*. In the first class, the chemical interactions between organic and inorganic compounds are weak (hydrogen, van der Waals or electrostatic interactions), while in a *class II*, the two phases are linked together through strong chemical covalent or coordinative bonds resulting in blends or interpenetrating networks [14,15]. Organic–inorganic hybrids can be prepared using varied synthetic strategies (e.g., sol gel route) that opens the possibility for the design of materials exhibiting tailored properties. This approach makes them suitable for several applications in: textile; packaging; construction; automobile industries; micro-optics; microelectronics; as well as in the synthesis of functional coatings; and as biosensors; biocatalysts or novel materials for cosmetics or biomedical purposes. Among them, adsorbents are one of the promising options [14,16–18].

Recently, there is a growing interest in the application of inexpensive adsorbents prepared from usable agricultural waste (e.g., egg shells, banana peels, rice husk) or common biopolymers such as alginate, gelatin, chitosan, lignocellulosic materials [6,19]. In the scientific literature there are several examples of gelatin application for the preparation of adsorbents [20–22]. Gelatin is a biodegradable, biocompatible and non-toxic natural polymer, widely used as a gelling agent in the manufacturing processes of food, cosmetic

components, and pharmaceuticals. Due to its good film-forming ability it can also be applied to the preparation of coatings or packaging materials [22,23]. However, due to its hydrophilic nature and high moisture sensitivity it requires modification (e.g., with cross-linking agents such as glutaraldehyde, phenolic acids, flavonoids, or genipin) in order to enhance mechanical and thermal stability. Physicochemical properties of gelatin can also be altered by the chemical reaction of a biopolymer with organosilicon compounds [24,25] or other biopolymers such as chitosan, alginate or polyvinyl alcohol [26–28]. Bajpai et al. [27] described adsorbers composed of gelatin, which reveals amphoteric nature due to the presence of both positive and negative charged centers (depending on its isoelectric point and pH of the environment) and anionic polymer alginate. They reported the pH of the effluent's dependent adsorption efficiency. In this work, we describe novel porous hybrid materials based on gelatin and organomodified silicone containing epoxy-group, which can be applied for adsorption of Cu(II), Cd(II) and Pb(II) from aqueous solution. To the best of our knowledge, this is the first report concerning gelatin–siloxane porous monoliths suitable for heavy metal removal. Gelatin was chemically modified in the reaction of its functional groups with the oxirane ring of a siloxane in order to enhance the stability in aqueous solutions of obtained adsorbers. As a result, porous gelatin–siloxane monoliths, containing amino groups ( $-\text{NH}_2$ ) and carboxyl groups ( $-\text{COOH}$ ), which can chelate with metal ions were obtained [29].

The aim of this work was to investigate the influence of organomodified siloxane amount used for the modification of gelatin on the adsorption properties of the gelatin–siloxane hybrid monoliths. Morphology, compressive strength and water absorption of hybrid monoliths were investigated. The effect of pH of aqueous solutions on metal ions adsorption was studied. Desorption tests were also performed.

## 2. Materials and Methods

### 2.1. Materials

Gelatin from porcine skin, type A (Bloom number 300, powder type) was purchased from Sigma-Aldrich and used as received. THF (tetrahydrofuran) was purchased from Avantor Performance Materials Poland S.A. and used as received. Poly(dimethyl-co-(methyl{3-(2,2,3,3,4,4,5,5-octafluoropentyloxy)propyl})-co-(methyl{3-glycidoxypropyl})) siloxane was synthesized according to methodology given by the authors elsewhere [30–32].

### 2.2. Gelatin–Siloxane Porous Hybrids Preparation

Gelatin–siloxane hybrids were prepared according to procedure, as described in detail elsewhere [24]. In a typical reaction, 2 g of gelatin were dissolved in water and heated under stirring. After complete dissolution of gelatin, a chosen amount of a siloxane, dissolved beforehand in THF, was added dropwise and the mixture was vigorously stirred for 5 h at the temperature in the range of 50–60 °C. Next, the temperature was raised to evaporate THF. When the solvent was completely removed, the reaction mixture was centrifuged to separate the synthesized hybrid. Next, the samples were frozen and freeze dried in order to completely remove the water. As a result, gelatin–siloxane porous hybrid monoliths with varied gelatin:siloxane mass ratios were obtained.

### 2.3. FT-IR Analysis

Fourier transform infrared spectroscopy analysis was performed using Spectrum 100 FT-IR Spectrometer (PerkinElmer) with an attenuated total reflection (ATR) accessory equipped with a diamond crystal, over a range of 4.000–400  $\text{cm}^{-1}$ .

### 2.4. SEM Analysis

Morphology of the samples was investigated using scanning electron microscopy (SEM). The analysis was carried out on a Zeiss Evo 40 instrument (Oberkochen, Germany). Prior to the examination all the samples were gold coated. SEM images were taken at the magnification of 250 $\times$ .

### 2.5. Compressive Strength of Gelatin and Gelatin–Siloxane Monoliths

The compressive strength was determined in order to assess the influence of siloxane incorporation on mechanical strength of gelatin. The test was performed using a 5.0 kN load cell of a universal tensile machine (Instron 5565) at a crosshead speed of 50 mm/min at room temperature. Investigated monoliths, with an average diameter of 25.5–26.0 mm and a height in the range of 8.5–9.0 mm, were examined at a compressing rate of 25 mm/min. Prior to the test, the diameter of each sample was measured in order to calculate the compressive strength (kPa) by dividing maximum load (N) by the surface area of each sample (mm<sup>2</sup>).

### 2.6. The Water Absorption

The water absorption ( $W_{abs}$ ) was evaluated using the following equation:

$$W_{abs}(\%) = \frac{W_t - W_0}{W_0} \cdot 100,$$

where  $W_0$  (g) is the mass of the monoliths before immersion into water and  $W_t$  (g) is the mass of gelatin monoliths after immersion. The monoliths were immersed in water for 10 h. Each experiment was performed three times.

### 2.7. Adsorption of Metal Ions

The adsorption performance of gelatin monoliths in relation to Pb(II), Cu(II) and Cd(II) was studied in batch mode. The experiments were carried out in 100 mL glass conical flask at ambient temperature. The gelatin monoliths were added to the sorbate solutions (20 mL) and shaken at 90 rpm. The concentration of metal was changing in the range 10 ppm to 100 ppm. The samples of aqueous solution (0.5 mL) were taken after the desired time (the contact time was varied from 3 to 60 h), diluted 10 times and centrifuged. The concentrations of metals ions were determined by atomic absorption spectroscopy (Varian AAS800). The measurements were carried out at 228.8 nm, 324.7 nm and 217.0 nm for cadmium(II), copper(II) and lead(II) ions, respectively. The initial pH of the sorbate solution was adjusted using 0.1 N HNO<sub>3</sub> solution. The pH of the solution was measured at the beginning and the end of each experiment using a pH meter (Thermo Scientific Orion Versa Star Pro 10, USA). The model solutions of copper(II), lead(II) and cadmium(II) were prepared from reagent grade salts received from POCh (Poland). Distilled water was used in all cases. The adsorption experiments were performed at a constant temperature (23.0 ± 1.0 °C).

The amount of adsorbed metal ions ( $q$ ), expressed in milligrams per gram (mg/g), was calculated according to the formula:

$$q = \frac{C_0 - C_t}{m} \cdot V$$

where:

$C_0$ -initial metal concentration, mg/L;

$C_t$ -metal concentration after time  $t$ , mg/L;

$m$ -mass of adsorbent, g;

$V$ -volume, dm<sup>3</sup>.

### 2.8. Investigation of pH Changes during Water Absorption

The experiment was carried out in 100 mL conical flasks containing 20 mL of distilled water. The gelatin monolith was introduced into the flask and mixed at agitation speed 90 rpm. The pH was measured after an appropriate time using a Thermo Scientific pH meter.

### 2.9. Desorption

Metal desorption experiments were performed for the selected gelatin monoliths in order to examine the reusability potential of these type of adsorbents. Hybrids (siloxane:gelatin mass ratio = 2:1), on which metal was previously adsorbed, were chosen for the investigation. Desorption process was carried out with distilled water for 10 h. Next, the concentration of metal in the obtained solution was measured using atomic absorption method. The monoliths, after desorption, were washed with distilled water and mineralized in a microwave oven (CEM MDS 2000) with a nitric acid. The solution obtained after mineralization was diluted and the concentration of the metal was measured. In the next step a mass balance of metal was calculated.

### 3. Results and Discussion

Gelatin was chemically modified in the reaction of its functional groups ( $-\text{NH}_2$  and  $-\text{COOH}$ ) with the oxirane ring of the organomodified siloxane (Figure 1): poly(dimethyl-co-(methyl{3-(2,2,3,3,4,4,5,5-octafluoropentyloxy)propyl})-co-(methyl,{3-glycidoxypropyl}) siloxane. All gelatin–siloxane hybrids were obtained in a form of porous, stiff monoliths (disc shaped). A representative hybrid denoted as GS 1:1 (gelatin:siloxane mass ratio 1:1) is presented in Figure 2.

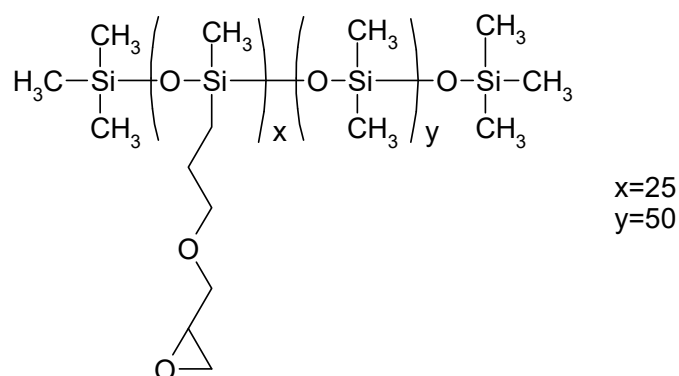


**Figure 1.** Chemical structure of the siloxane.



**Figure 2.** Photograph of the gelatin–siloxane hybrid GS 1:1 (gelatin:siloxane mass ratio 1:1).

#### 3.1. FT-IR Analysis of Gelatin and Gelatin–Siloxane Monoliths

FT-IR spectra of unmodified gelatin and representative gelatin–siloxane hybrid are presented in Figure 3. In the case of gelatin, the results confirmed the presence of characteristic peaks at  $3290$  and  $1533\text{ cm}^{-1}$  representing NH stretching and bending vibrations (amid II), respectively, at  $1635\text{ cm}^{-1}$  bands associated with stretching vibration of the  $\text{C}=\text{O}$

(amide I), and at  $1245\text{ cm}^{-1}$  for the stretching vibration of the C–N band (amide III) corresponding to the triple helix structure of gelatin [33]. The FT-IR spectra of gelatin-siloxane hybrid showed the presence of the bands characteristic for siloxane at  $2965\text{ cm}^{-1}$  (C–H) as well as at  $1270\text{ cm}^{-1}$  attributed to the vibrations of Si–CH<sub>3</sub>, which were introduced to the biopolymer in a chemical reaction of gelatin functional groups (–NH<sub>2</sub> and –COOH) with the oxirane ring of the organomodified siloxane. Moreover, characteristic bands at  $1160\text{ cm}^{-1}$ , revealing the presence of Si–O–Si bonds, were observed.

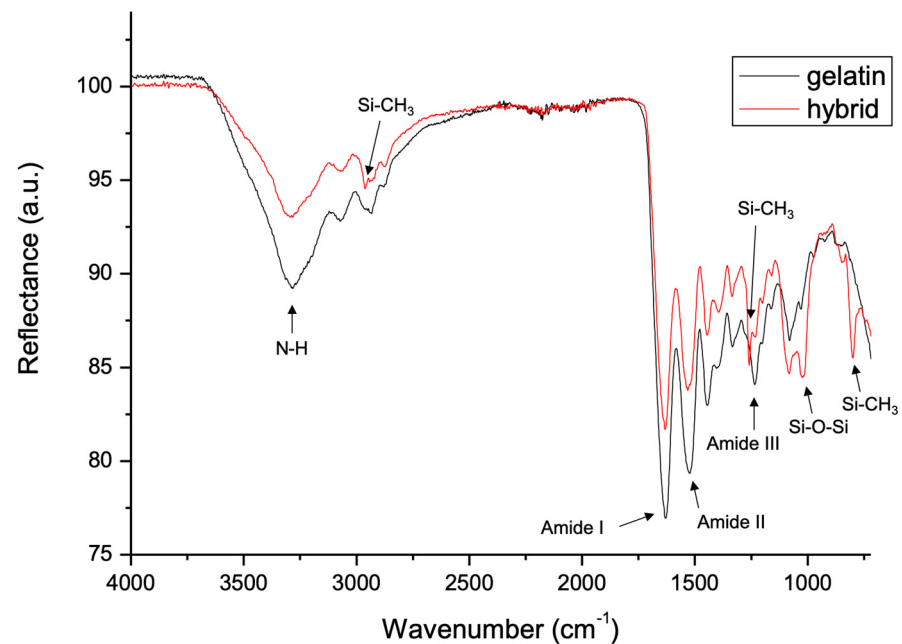


**Figure 3.** FTIR spectra of unmodified gelatin and gelatin-siloxane hybrid (GS 1:1).

### 3.2. SEM Analysis of Gelatin and Gelatin-Siloxane Monoliths

SEM images of cross-section surfaces of analyzed samples obtained with magnification of  $250\times$  are presented in Figure 4. In case of the unmodified gelatin and the gelatin-siloxane hybrid, a typical foam like structure with interconnected pores were observed. The sizes of the pores for neat biopolymer were in the range of  $60\text{--}200\text{ }\mu\text{m}$ , while for hybrid material the range was  $80\text{--}400\text{ }\mu\text{m}$ .

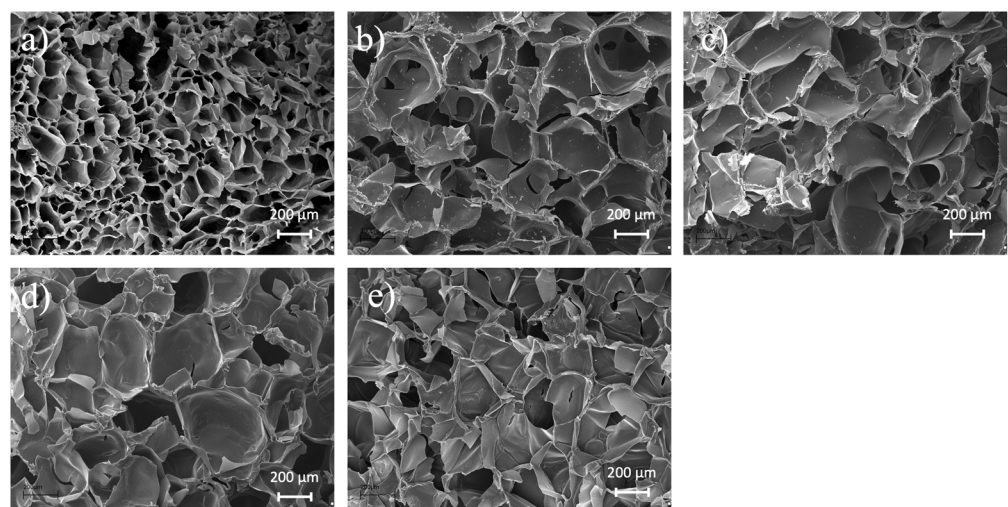


**Figure 4.** SEM images of the lyophilized samples: (a) unmodified gelatin, (b) gelatin-siloxane hybrid GS 1:1, (c) GS 2:1, (d) G:S 3:1, (e) GS 4:1.

### 3.3. Compressive Strength Results

Compressive strength results are presented in Table 1.

**Table 1.** Compressive strength of gelatin (G) and gelatin–siloxane monoliths (GS).

| Sample | Compressive Strength (kPa) |
|--------|----------------------------|
| G      | 206.3 ± 18.6               |
| GS 1:1 | 157.1 ± 3.2                |
| GS 2:1 | 184.6 ± 13.5               |
| GS 3:1 | 190.2 ± 2.4                |
| GS 4:1 | 197.5 ± 5.2                |

The data presented in the Table 1 shows that the addition of siloxane has an influence on the mechanical properties of porous monoliths. It was observed that the introduction of siloxane into biopolymer matrix enhanced the flexibility of the porous monoliths. The higher the amount of the siloxane, the more pronounced the reduction in their compression strength when compared to the unmodified gelatin. In the case of the hybrid GS 1:1 the examined parameter was lower by about 25%. The results of the compressive strength test correspond to the morphology investigation since SEM images revealed wider pores in the case of the gelatin–siloxane hybrids and more dense structure with smaller pores for unmodified gelatin.

### 3.4. The Water Absorption

A water absorption study was performed for unmodified gelatin as well as for hybrid monoliths, however samples prepared from unmodified biopolymer disintegrated in water into small parts at the beginning of the test and a precise calculation was impossible in this case. On the contrary, it was observed that hybrids obtained with gelatin:siloxane mass ratios 1:1 and 2:1 did not fall into pieces during the performed procedure. Therefore, the results showed that the chemical modification of biopolymer with an appropriate amount of the siloxane resulted in an enhanced stability in aqueous solutions of the hybrid adsorbents. The water absorption of gelatin–siloxane monoliths was about 1800% for GS 1:1 and 1900% for GS 2:1. The obtained values are similar to the results described by Zhang et al. [34]. They observed 1700% of water absorption in case of porous chitosan–gelatin monoliths, as well as 2700% and 3100% when 1% and 4% of grafene oxide was incorporated into the monoliths, respectively. They assume that the increase in water absorption is due to the presence of hydroxyl and carboxyl groups on grafene oxide, which increase the hydrophilicity and water permeability of porous monoliths and participate in electrostatic interactions with chemical groups of chitosan. In case of the hybrid monoliths described in this study, the varied content of siloxane did not essentially affect water absorption values. This is probably due to the fact that functional groups of the siloxane have reacted with gelatin as well as the hydrophobic nature organomodified silicone. Interestingly, we also observed changes in the shape and size of the gelatin monoliths, which significantly increased their volume. Notably, the hybrid monoliths GS 1:1 started to disintegrate after two days of soaking in solution during shaking and after six days without shaking, which is similar to chitosan–gelatin monoliths' stability (five days) described by Zhang et al. [34]. It means that gelatin–siloxane monoliths show similar wet-strength and wet-state stability to chitosan–gelatin monoliths. Therefore, in order to investigate the resistance of hybrid adsorbents, further experiments were performed with various types of immersion liquid as well as various amount of the siloxane incorporated into gelatin matrix.

### 3.5. Resistance of Gelatin Beads to Shaking in Water Solutions

Gelatin–siloxane monoliths modified with different amounts of the siloxane were tested in order to determine the disintegration time in immersion liquid. The results of the resistance test are shown in Table 2. The monoliths used for the experiment were synthesized using the following mass ratios of gelatin to siloxane: 1:1, 2:1, 3:1, 4:1, 6:1, and 8:1.

The gelatin–siloxane monoliths were immersed and shaken in: 100 mg/L copper aqueous solution and in distilled water. All samples were shaken under identical conditions.

**Table 2.** The disintegration time of gelatin–siloxane monoliths.

| Type of Solution | Composition of Hybrid Monoliths (Gelatin:Siloxane) | pH      |           |           | Disintegration Time [hours] |
|------------------|--|---------|-----------|-----------|-----------------------------|
|                  |  | Initial | After 1 h | After 2 h |                             |
| Cu(II)           | 1:1  | 2.26    | -         | -         | >48                         |
| Cu(II)           | 2:1  | 2.26    | -         | -         | >24                         |
| Cu(II)           | 3:1  | 2.26    | 4.58      | 6.01      | 8                           |
| Cu(II)           | 4:1  | 2.26    | 4.47      | 5.82      | 6                           |
| Cu(II)           | 6:1  | 2.26    | 6.15      | 6.98      | 2                           |
| Cu(II)           | 8:1  | 2.26    | 4.42      | 5.78      | 3                           |
| water            | 4:1  | 5.05    | 9.64      | 9.57      | 5                           |
| water            | 6:1  | 5.05    | 9.77      | 9.69      | 2                           |
| water            | 8:1  | 5.05    | 9.73      | 9.70      | 2                           |

The obtained results showed that regardless what type of initial immersion liquid used (water or metal ion solution with pH adjusted by HCl) the resistance time, after which gelatin monoliths started to decompose into smaller pieces, depends on the siloxane content. The lower the content, the faster disintegration takes place. Graphical illustration showing the effect of the siloxane addition on the stability of gelatin monoliths, measured with agitation speed of 90 rpm, is shown in Figure 5.

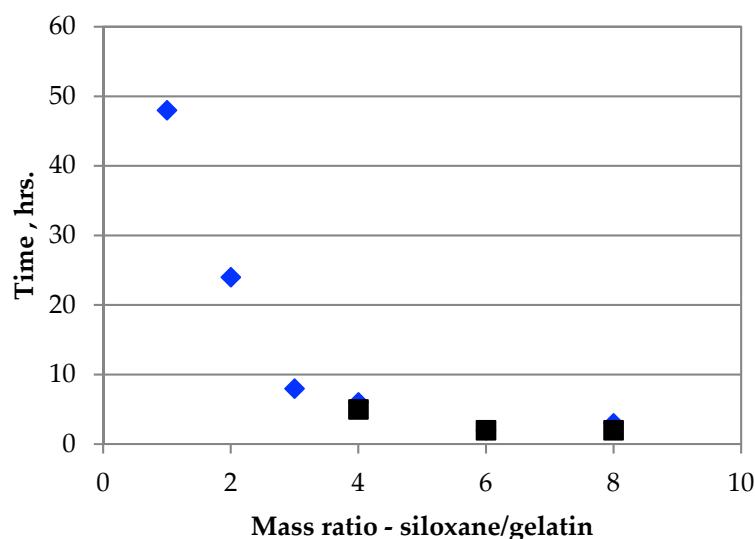


**Figure 5.** Stability of the monolith depending on the mass ratio of gelatin to siloxane, (◆—copper, ■—distilled water), measured with agitation speed of 90 rpm.

### 3.6. The Adsorption of Heavy Metals ( $\text{Cu}^{2+}$ , $\text{Pb}^{2+}$ , $\text{Cd}^{2+}$ ) on the Gelatin Monoliths

#### 3.6.1. Effect of Contact Time

Information on the kinetics of metal uptake is crucial for the selection of appropriate conditions for batch metal removal process. The adsorption rate of copper, lead and cadmium ions was investigated. The adsorption rates of these metal ions on studied hybrids were rather slow and within 3 h about 50% of the metal ions in solution was removed (Figure 6). In the case of the gelatin–siloxane monolith GS 1:1, the rate of metal adsorption is much lower (Figure 7). It was observed that the rate of Cd(II), Cu(II) and Pb(II) adsorption depends on the agitation speed, however too vigorous agitation may lead to the destruction of hybrid monoliths. Therefore, the stirring speed was limited to 90 rpm to avoid rapid disintegration of the monoliths. Figure 7 shows the concentrations of metals

in aqueous solutions measured after adsorption on gelatin–siloxane hybrid GS 1:1. The study was carried out to determine the time when the process would reach equilibrium. Measurements were made after 3, 5, 9, 12, 15 and 18 h of shaking the samples. The obtained results clearly showed that the adsorption occurs quickly in the initial period and then the process slows down. It was also observed that the adsorption of metals ions in the studied period of time is higher for GS 2:1 in comparison to GS 1:1. The experiments were completed after 18 h to avoid the breakdown of hybrid monoliths. A slight decrease in adsorption observed for GS 2:1 in case of lead and cadmium after 18 h of shaking may indicate the beginning of the monoliths' disintegration, although there were no visible changes in their structure. A decrease in adsorption was not observed for the GS 1:1 hybrid, probably due to its higher stability in aqueous solutions (see Table 2).

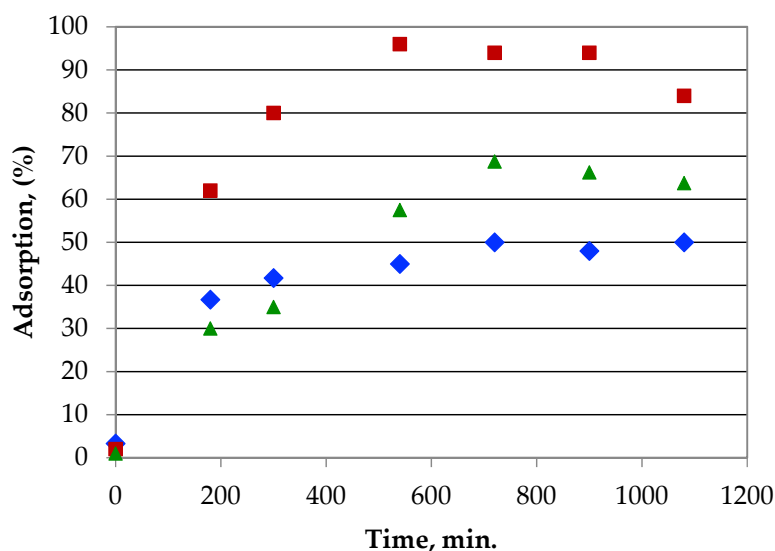


**Figure 6.** Effect of contact time on the adsorption of Cu(II) (◆), Pb(II) (■) and Cd(II) (▲) on gelatin–siloxane monoliths GS 2:1 (initial concentration of metals–10 mg/L; initial pH = 2.6; agitation speed–90 rpm; mass of adsorbent monoliths  $0.32 \pm 0.02$  g; temperature  $23 \pm 1.0$  °C).

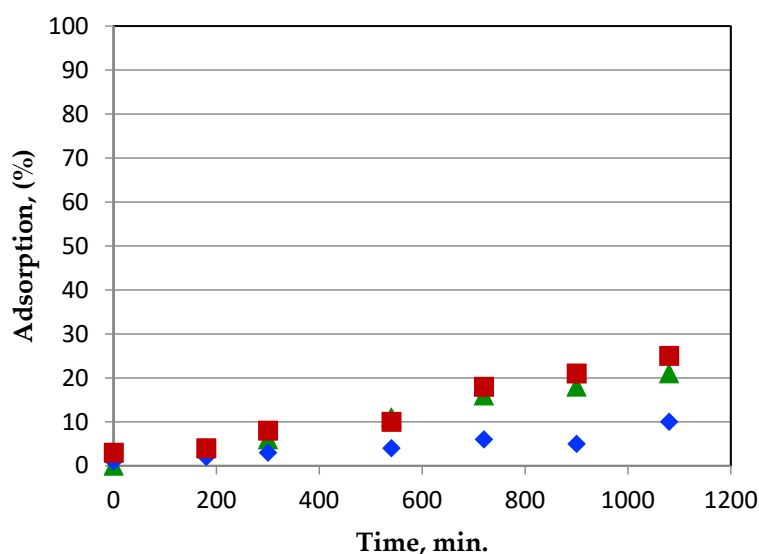


**Figure 7.** Effect of contact time on the adsorption of Cu(II) (◆), Pb(II) (■) and Cd(II) (▲) on gelatin–siloxane monoliths GS 1:1 (initial concentration of metals–10 mg/L; initial pH = 2.6; agitation speed–90 rpm; mass of adsorbent monoliths  $0.32 \pm 0.02$  g; temperature  $23 \pm 1.0$  °C).

Figure 8 shows the photos of hybrid monoliths after the adsorption process (18 h) for each studied metal ion. The color of the monolith after copper adsorption was intense blue and no changes were observed in the case of adsorption of other metals.

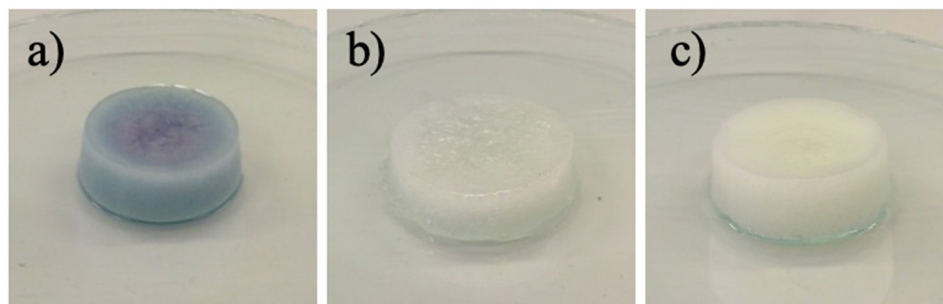


**Figure 8.** Photographs of the GS 2:1 hybrids after adsorption of metal ions: (a) copper(II), (b) lead(II), (c) cadmium(II).

### 3.6.2. pH Changes during Metal Adsorption

pH is an important factor affecting the performance of the metal ion sorption process, which can affect both the form of the metal ion in the solution and the surface properties of the sorbent. The latter is dependent on the competition between metal ions and protons in available binding sites or results from ion exchange. We examined the influence of contact time on the pH of solutions during adsorption. The results are presented in Figure 9. Typically, during the adsorption process of metal ions the concentration of hydrogen ions increases however, in our studies, we observed that the solution became more basic. Such behavior is due the sodium carbonate used for the synthesis of hybrid monoliths. During the experiment sodium carbonate was leached from the hybrids and changed pH. Therefore, the initial pH value was controlled and adjusted during the metal adsorption process. In order to avoid the precipitation of metal hydroxides, which can occur when the pH of the solution is too high, 0.1 M of HNO<sub>3</sub> was added to the metal solutions before adsorption experiment. Lowering the initial pH to 2.6 resulted in a reduction in the final pH to about 5-6. This value was sufficient to avoid the precipitation of metal hydroxides. On the other hand, if the initial pH was too low, rapid destruction of the monoliths was observed.

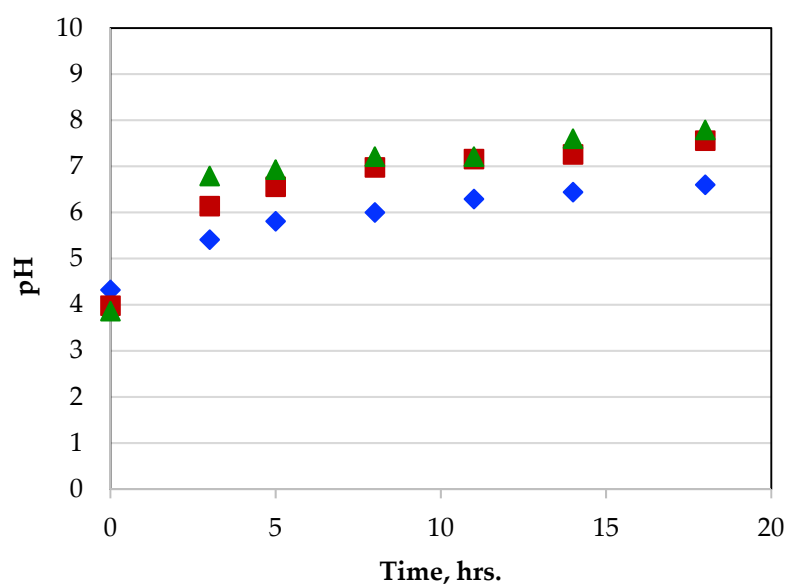


**Figure 9.** Effect of contact time on the pH of solutions during adsorption of Cu(II) (◆), Pb(II) (■) and Cd(II) (▲) by hybrid monoliths GS 2:1: initial Cu(II) concentration 10 ppm, mass of adsorbent monoliths  $0.32 \pm 0.02$  g, initial pH 4 and temperature  $23 \pm 1$  °C.

### 3.6.3. Adsorption Kinetics of Metal Ions on Gelatin–Siloxane Monoliths

The adsorption kinetics of studied metal ions was analyzed by the use of pseudo-first-order kinetic models and pseudo-second-order kinetic models [19,29,35]. The pseudo-first-order adsorption model can be expressed as:

$$\log(q_e - q) = \log q_e - k_1 \cdot t$$

where  $q_e$  (mg/L) denotes the amount of metal ions adsorbed at equilibrium,  $q$  (mg/L) the amount of metal ions adsorbed (mg/L) at time  $t$  (min) and  $k_1$  denotes the rate constant (1/min). The pseudo second-order adsorption model can be expressed as:

$$\frac{t}{q_t} = \frac{1}{k_2 q_e^2} + \frac{1}{q_e} \cdot t$$

where  $q_e$  and  $q_t$  are the amount of metal ions adsorbed per unit mass of the adsorbent (mg/g) at equilibrium time and time  $t$ , respectively, and  $k_1$  is the rate constant for the second-order kinetics. After the linearization of above equations rate constants ( $k_1, k_2$ ), maximum adsorption capacity ( $q_e$ ) and correlation coefficients ( $R^2$ ) for pseudo-first order and the pseudo-second order equations values were calculated (Table 3).

**Table 3.** The adsorption rate constants ( $k_1, k_2$ ), maximum adsorption capacity ( $q_e$ ) and correlation coefficients ( $R^2$ ) for pseudo-first order and pseudo-second order equations.

| Metal Ions | Pseudo-First Order         |               |       | Pseudo-Second Order |               |       |
|------------|----------------------------|---------------|-------|---------------------|---------------|-------|
|            | $k_1$<br>min <sup>-1</sup> | $q_e$<br>mg/g | $R^2$ | $k_2$<br>g/(mg min) | $q_e$<br>mg/g | $R^2$ |
| GS 2:1     |                            |               |       |                     |               |       |
| Cu         | 0.00568                    | 0.893         | 0.915 | 4.389               | 1.045         | 0.993 |
| Pb         | 0.00564                    | 1.92          | 0.974 | 1.340               | 1.892         | 0.978 |
| Cd         | 0.00231                    | 1.33          | 0.968 | 1.910               | 1.584         | 0.915 |
| GS 1:1     |                            |               |       |                     |               |       |
| Cu         | 0.00104                    | 0.449         | 0.989 | 12.040              | 0.631         | 0.902 |
| Pb         | 0.00216                    | 0.726         | 0.968 | 9.398               | 0.902         | 0.856 |
| Cd         | 0.00122                    | 0.516         | 0.951 | 8.294               | 0.760         | 0.714 |

The values in Table 3 show that both the first- and the second-order pseudo kinetic models can fit the concentration profiles, however correlation coefficients are lower for second-order model ( $R^2 > 0.92$ ).

### 3.6.4. The Effect of Metal Ions Concentration

The effect of metal ions concentration on adsorption is shown in Figure 10. The effect of the initial concentration of metal ions on the adsorption efficiency was tested at the adsorbent dose of  $0.4 \pm 0.02$  g. Due to the less effective adsorption of metal ions on the hybrid GS 1:1 further experiments and calculations were made only for the GS 2:1 hybrid monolith. The results confirmed that the increase in the initial concentration of metal ions had a positive effect on their adsorption and resulted in the increased amount of the adsorbed metal. This phenomenon can be explained by the fact that the adsorption capacity increased as there were still enough active sites on hybrid monoliths to fill.

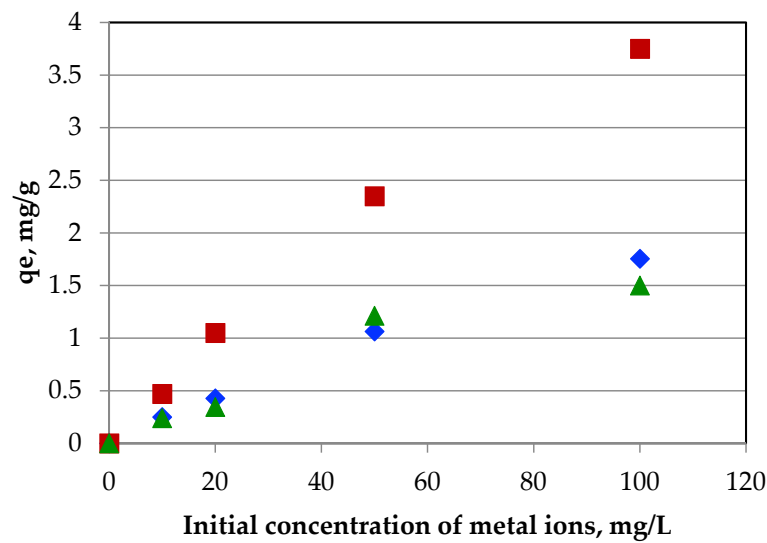


**Figure 10.** Adsorption isotherms of Cu(II) (◆), Pb(II) (■) and Cd(II) (▲) ions onto hybrid monolith GS 2:1; dose  $0.4 \pm 0.02$  g/20 mL, temperature  $23 \pm 1$  °C, initial pH 2.3 and equilibrium time 10 h.

Langmuir and Freundlich adsorption isotherm models were used to describe the adsorption of studied metals ions on gelatin–siloxane monoliths. The Langmuir isotherm is given by the following equation [35]:

$$q_e = \frac{q_{max} \cdot K_L \cdot C_e}{1 + K_L \cdot C_e}$$

where  $q_e$  (mg/g) is the equilibrium adsorption capacity;  $q_{max}$  (mg/g) -the maximum adsorption capacity;  $K_L$ -the Langmuir constant;  $C_e$  [mg/L]-the equilibrium concentration after the adsorption process. The Freundlich isotherm is given by equation:

$$q_e = K_F C_e^{\frac{1}{n}}$$

where  $q_e$  (mg/g) and  $C_e$  (mg/L),  $K_F$ - the Freundlich constant and  $1/n$ -the intensity of adsorption.

The Langmuir and Freundlich isotherm constants with the correlation coefficients are shown in Table 4.

**Table 4.** Isotherm model constants and correlation coefficients for metal ions adsorption.

| Metal Ions | pH | Langmuir Isotherm |               |       | Freundlich Isotherm |                                |       |
|------------|----|-------------------|---------------|-------|---------------------|--------------------------------|-------|
|            |    | $q_{max}$<br>mg/g | $K_L$<br>L/mg | $R^2$ | $K_F$<br>mg/g       | $n$<br>(L/mg) <sup>(1/n)</sup> | $R^2$ |
| Cu         |    | 2.688             | 0.0193        | 0.938 | 0.4720              | 5.5889                         | 0.971 |
| Pb         |    | 3.500             | 0.2507        | 0.849 | 0.7111              | 2.0151                         | 0.909 |
| Cd         |    | 3.088             | 7.9000        | 0.877 | 0.1816              | 6.5908                         | 0.817 |

The Langmuir model describes the maximum adsorption of metal ions on completely homogeneous surface with negligible interaction between adsorbed molecules. The values of  $q_{max}$  and  $K_L$  were calculated to be 2.69 and 0.0193 (Cu), and 3.5 and 0.2507 (Pb) and 3.09 and 7.9 (Cd), respectively. The adjustment of the isotherm to the experimental data is not very good as indicated by the correlation coefficient values ( $R^2$ ), which range from 0.849 to 0.938.

The Freundlich  $K_F$  and  $n$  constants were estimated from 0.1816 to 0.7111 and from 2.015 to 6.591. Based on the obtained results, data are assumed to be more in line with the Freundlich model.

It is particularly important to compare adsorption capacity of obtained hybrid monoliths with the values denoted for other adsorbents, also based on the biopolymers. Experimental maximum adsorption capacity for hybrid monoliths was 3.75 mg/g for Pb(II), 1.76 mg/g for Cu(II) and 1.5 mg/g for Cd(II). The comparison of the maximum adsorption capacity of studied metals onto various adsorbents described in the literature is presented in Table 5. It indicates that the samples examined in this work show lower values in comparison to many other adsorbents, including some gelatin-based ones [32–47]. In case of chitosan–gelatin monoliths reinforced with graphite oxide nanosheets (GO), reported by Zhang et al. [34], the adsorption capacity measured for Pb(II) and Cu(II) was 100 mg/g and 130 mg/g, respectively. In both cases, the addition of GO nanosheets improved the strength of chitosan–gelatin adsorbents and provided a great number of functional groups that allow for the binding with metal ions. Comparable values of adsorption capacity were reported for olive stone, pomegranate peel, bael tree leaf powder and monolithic xerogel [41–43,45]. However, despite the fact that adsorption capacity values for hybrid adsorbents tested in this study are not very high, it should be underlined that their preparation is easy and cost-effective.

**Table 5.** The comparison of adsorption capacity of studied metal ions onto various adsorbents.

| Adsorbent  | $q_m$ , mg/g | Metal  | Reference    |
|--|--------------|--------|--------------|
| CGGO (chitosan-gelatin/graphene oxide) monoliths       | about 100    | Pb(II) | [34]         |
|  | about 130    | Cu(II) |              |
| Granular activated carbon                              | 26.546       | Pb(II) | [35]         |
| Fly ash  | 51.98        | Pb(II) | [36]         |
| Green algae Spirogyra                                  | 90.91        | Pb(II) | [37]         |
|  | 38.61        | Cu(II) |              |
| Chitosan crosslinked with epichlorohydrin triphosphate | 130.72       | Cu(II) | [38]         |
|  | 83.72        | Cd(II) |              |
|  | 166.94       | Pb(II) |              |
| PVA/gelatin hydrogel beads                             | 211.86       | Pb(II) | [29]         |
| PVA/CS/GO hydrogel beads                               | 162          | Cu(II) | [39]         |
| Fly-ash-based SBA-15                                   | 131.00       | Pb(II) | [40]         |
| Olive stone  | 5.88         | Pb(II) | [41]         |
|  | 7.33         | Cd(II) |              |
| Bael tree leaf powder                                  | 4.065        | Pb(II) | [42]         |
| Pomegranate peel                                       | 1.32         | Cu(II) | [43]         |
| Pink bark  | 11.94        | Cu(II) | [44]         |
| Monolithic xerogel                                     | 0.585        | Cu(II) | [45]         |
| Silica gel with SGA                                    | 0.22 mmol/g  | Cu(II) | [46]         |
| Magnetic nanocomposites                                | 4.11         | Cd(II) | [47]         |
| Silica-Coated Magnetic Nanocomposites                  | 14.9         | Pb(II) | [48]         |
| Gelatin-siloxane monoliths                             | 3.75         | Pb(II) | own research |
|  | 1.76         | Cu(II) |              |
|  | 1.5          | Cd(II) |              |

### 3.7. Desorption of Metals Ions

An effective adsorbent for removing metal ions should not only show a good adsorption capacity but also allow for desorption of metal ions, which is desirable from economic and ecological point of view. For this reason, we investigated the desorption of Cu(II), Pb(II) and Cd(II) ions from loaded monoliths. Several studies have shown that HCl, HNO<sub>3</sub> and H<sub>2</sub>SO<sub>4</sub> are effective in desorbing of heavy metals from loaded adsorbents [49]. In our study 0.1 M HCl was initially used for desorption but such a stripping agent caused a rapid destruction of the hybrid monoliths. Therefore, distilled water was used for further experiments. The desorption process was carried out for 10 h. Unfortunately, also under these conditions, only few of the monoliths were not disintegrated into small pieces. After this time, the observed level of desorption was in the range of 26–69%. To verify the correctness of the experiment, after the desorption process, the remaining monolith was separated from the solution and washed with distilled water. Next, the microwave oven digestion was employed for the determination of metal ions remained in monoliths. The sample after mineralization was diluted with distilled water to a specific volume and the concentration of metals was measured. Then, the amounts of copper and cadmium in the adsorption and desorption process were compared. The results are shown in Table 6. Mass balance was calculated using data denoted in columns three and six (Table 6), according to the equation provided in column seven.

**Table 6.** Mass balance of adsorption and desorption processes (GS 2:1, [Cu]<sub>0</sub> = 9.61 mg/L, [Cd]<sub>0</sub> = 9.91 mg/L, [Pb]<sub>0</sub> = 10.01 mg/L, initial pH = 2.6).

| Metal  | Adsorption Process           |                                       |  | Desorption Process                    |                                  | Mass Balance          |                |
|--------|------------------------------|---------------------------------------|--|---------------------------------------|----------------------------------|-----------------------|----------------|
|        | 1                            | 2                                     | 3  | 4                                     | 5                                | 6                     | 7              |
|        | Initial Amount of Metal Ions | Amount of Metal ions after Adsorption | Amount of Metal Adsorbed (Difference between Column 1 and 2) | Amount of Metal Ions After Desorption | Amount of Metal Ions in Monolith | Sum of Column 4 and 5 | (3-6)/3 × 100% |
|        | µg                           | µg                                    | µg   | µg                                    | µg                               | µg                    | %              |
| Cd(II) | 192.6                        | 30.2                                  | 162.4  | 38.6                                  | 110.5                            | 149.1                 | 8.2            |
| Cu(II) | 198.2                        | 87.2                                  | 111.0  | 65.8                                  | 30.2                             | 95.8                  | 13.7           |
| Pb(II) | 200.2                        | 18.2                                  | 182.0  | 107.4                                 | 58.3                             | 165.7                 | 9.0            |

A satisfactory agreement between mass of metal adsorbed and desorbed was observed for each considered metal. The mass balance of Cd(II) and Cu(II) determined as the difference between the initial amount of metal in the aqueous phases and after adsorption agreed with the contents of these species in the aqueous phase after desorption and adsorbed in gelatin hybrid with an error of 8.2–13.7%. In light of the above, it can be stated that hybrid monoliths are promising biopolymer-based novel adsorbents. The results showed that in the case of hybrid monoliths that are stable in aqueous solutions prepared with a desired amount of the siloxane, the desorption of metal ions can reach 70%.

## 4. Conclusions

Novel, gelatin–siloxane porous monoliths were successfully prepared in the chemical reaction of gelatin with organomodified silicone and applied for the purpose of heavy metals removal. The results showed that the incorporation of the siloxane into the gelatin matrix resulted in an enhanced stability of the hybrid monoliths, in comparison with the unmodified gelatin, which disintegrated in aqueous solutions. It was confirmed that obtained hybrid monoliths can be applied for adsorption of Cu(II), Cd(II) and Pb(II) from aqueous solutions. Parameters for the most effective heavy metal removal such as gelatin:siloxane composition, contact time and pH values of the immersion liquid were determined. The desorption of metal ions for hybrid monoliths stable in aqueous solutions reached 70%. The future scope of the work is to conduct further experiments with gelatin–siloxane porous monoliths obtained with a unidirectional freeze-drying procedure in order to investigate the influence of the resulted morphology of the porous samples on the heavy metal adsorption properties. Also, other types of siloxanes are intended to be applied for the modification

of gelatin in order to examine their potential for preparation of gelatin-siloxane hybrids suitable for heavy metal removal.

**Author Contributions:** P.W., R.C. and H.M.; methodology, P.W., R.C. and H.M.; investigation, P.W. and R.C.; writing-original draft preparation, P.W. and R.C.; manuscript revision, H.M.; All authors have read and agreed to the published version of the manuscript.

**Funding:** This research received no external funding.

**Institutional Review Board Statement:** Not applicable.

**Informed Consent Statement:** Not applicable.

**Data Availability Statement:** Not applicable.

**Conflicts of Interest:** The authors declare no conflict of interest.

## References

1. Fu, F.; Wang, Q. Removal of Heavy Metal Ions from Wastewaters: A Review. *J. Environ. Manag.* **2011**, *92*, 407–418. [[CrossRef](#)] [[PubMed](#)]
2. Gupta, V.K.; Moradi, O.; Tyagi, I.; Agarwal, S.; Sadegh, H.; Shahryari-Ghoshekandi, R.; Makhlof, A.S.H.; Goodarzi, M.; Garshasbi, A. Study on the removal of heavy metal ions from industry waste by carbon nanotubes: Effect of the surface modification: A review. *Crit. Rev. Environ. Sci. Technol.* **2016**, *46*, 93–118. [[CrossRef](#)]
3. Demirbas, A. Heavy metal adsorption onto agro-based waste materials: A review. *J. Hazard. Mat.* **2008**, *157*, 220–229. [[CrossRef](#)] [[PubMed](#)]
4. Ishanullah, A.A.; Al-Amer, A.M.; Laoui, T.; Al-Marri, M.J.; Nasser, M.S.; Khraisheh, M.; Atieh, M.A. Heavy metal removal from aqueous solution by advanced carbon nanotubes: Critical review of adsorption applications. *Sep. Purif. Technol.* **2016**, *157*, 141–161. [[CrossRef](#)]
5. Kurniawan, T.A.; Chan, G.Y.S.; Loa, W.-H.; Babel, S. Physico-Chemical Treatment Techniques for Wastewater Laden with Heavy Metals. *Chem. Eng. J.* **2006**, *118*, 83–98. [[CrossRef](#)]
6. Kumar, M.; Seth, A.; Singh, A.K.; Rajput, M.S.; Sikandar, M. Remediation strategies for heavy metals contaminated ecosystem: A review. *Environ. Sustain. Indic.* **2021**, *12*, 100155. [[CrossRef](#)]
7. Lakherwal, D. Adsorption of Heavy Metals: A Review. *Inter. J. Environ. Res. Dev.* **2014**, *4*, 41–48.
8. Babel, S.; Kurniawan, T.A. Low Cost Adsorbents for Heavy Metals Uptake from Contaminated Water: A Review. *J. Hazard. Mat.* **2003**, *B97*, 219–243. [[CrossRef](#)]
9. Hasanpour, M.; Hatami, M. Application of three dimensional porous aerogels as adsorbent for removal of heavy metal ions from water/wastewater: A review study. *Adv. Colloid Inter. Sci.* **2020**, *284*, 102247. [[CrossRef](#)]
10. Li, J.; Li, X.; Alsaedi, A.; Hayat, T.; Chen, C. Synthesis of highly porous inorganic adsorbents derived from metal-organic frameworks and their application in efficient elimination of mercury(II). *J. Colloid Interf. Sci.* **2018**, *517*, 61–71. [[CrossRef](#)]
11. Sanchez, C.; Lebeau, B.; Chaput, F.; Boilot, J.-P. Optical Properties of Functional Hybrid Organic-Inorganic Nanocomposites. *Adv. Mater.* **2003**, *15*, 1969–1994. [[CrossRef](#)]
12. Pandey, S.; Mishra, S.B. Sol-gel derived organic-inorganic hybrid materials: Synthesis, characterizations and applications. *J. Sol-Gel Sci. Technol.* **2011**, *59*, 73–94. [[CrossRef](#)]
13. IUPAC. *Compendium of Chemical Terminology*, 2nd ed.; the “Gold Book”; McNaught, A.D., Wilkinson, A., Eds.; Online Version 2019; Chalk, S.J., Created; Blackwell Scientific Publications: Oxford, UK, 1997; ISBN 0-9678550-9-8. [[CrossRef](#)]
14. Kickelbick, G. *Hybrid Materials: Synthesis, Characterization, and Applications*; WILEY-VCH Verlag GmbH & Co. KGaA: Weinheim, Germany, 2007.
15. Sanchez, C.; Julian, B.; Belleville, P.; Popall, M. Application of Hybrid Organic-Inorganic Nanocomposites. *J. Mat. Chem.* **2005**, *15*, 3559–3592. [[CrossRef](#)]
16. Drisko, G.L.; Sanchez, C. Hybridization in Materials Science—Evolution, Current State, and Future Aspirations. *Eur. J. Inorg. Chem.* **2012**, *32*, 5097–5105. [[CrossRef](#)]
17. Tsuru, K.; Hayakawa, S.; Osaka, A. Synthesis of Bioactive and Porous Organic-Inorganic Hybrids for Biomedical Applications. *J. Sol-Gel Sci. Technol.* **2004**, *32*, 201–205. [[CrossRef](#)]
18. Wang, S.; Kang, Y.; Wang, L.; Zhang, H.; Wang, Y.; Wang, Y. Organic/inorganic hybrid sensors: A review. *Sens. Actuators B* **2013**, *182*, 467–481. [[CrossRef](#)]
19. Obanla, O.R.; Mohammed, F.U.; Ojewumi, M.E.; Odunlami, O.A.; Ikpotor, U.F. Kinetic Adsorption of Heavy Metal (Copper) On Rubber (*Hevea Brasiliensis*) Leaf Powder. *S. Afr. J. Chem. Eng.* **2021**, *37*, 74–80.
20. Wahlström, N.; Steinhagen, S.; Toth, G.; Pavia, H.; Edlund, U. Ulvan dialdehyde-gelatin hydrogels for removal of heavy metals and T methylene blue from aqueous solution. *Carbohydr. Polym.* **2020**, *249*, 116841. [[CrossRef](#)]

21. Marciano, J.S.; Ferreira, R.R.; de Souza, A.G.; Barbosa, R.F.S.; de Moura Junior, A.J.; Rosa, D.S. Biodegradable gelatin composite hydrogels filled with cellulose for chromium (VI) adsorption from contaminated water. *Int. J. Biol. Macromol.* **2021**, *181*, 112–124. [[CrossRef](#)]
22. Kamal, O.; Pochat-Bohatier, C.; Sanchez-Marcano, J. Development and stability of gelatin cross-linked membranes for copper (II) ions removal from acid waters. *Sep. Purif. Technol.* **2017**, *183*, 153–161. [[CrossRef](#)]
23. Wojciechowska, P.; Tichoniuk, M.; Gwiazdowska, D.; Maciejewski, H.; Nowicki, M. Antimicrobial activity of organic–inorganic hybrid films based on gelatin and organomodified silicones. *Adv. Polym. Technol.* **2018**, *37*, 2958–2970. [[CrossRef](#)]
24. Wojciechowska, P.; Pietras, P.; Maciejewski, H. Synthesis, Characterization, and Thermal Properties of Organic–Inorganic Hybrids Based on Gelatin and Organomodified Silicones. *Adv. Polym. Technol.* **2014**, *33*, 21459. [[CrossRef](#)]
25. Zhang, M.; Wu, Y.; Zhang, Q.; Xia, Y.; Li, T. Synthesis and characterization of gelatin-polydimethylsiloxane graft copolymers. *J. Appl. Polym. Sci.* **2011**, *120*, 2130–2137. [[CrossRef](#)]
26. Cui, L.; Xiong, Z.; Guo, Y.; Liu, Y.; Zhao, J.; Zhang, C.; Zhu, P. Fabrication of interpenetrating polymer network chitosan/gelatin porous materials and study on dye adsorption properties. *Carbohydr. Polym.* **2015**, *132*, 330–337. [[CrossRef](#)] [[PubMed](#)]
27. Bajpai, J.; Shrivastava, R.; Bajpai, A.K. Dynamic and equilibrium studies on adsorption of Cr(VI) ions onto binary bio-polymeric beads of cross linked alginate and gelatin. *Colloids Surf. A Physicochem. Eng. Asp.* **2004**, *236*, 81–90. [[CrossRef](#)]
28. Murilo, Á.; Rodrigues, V.; Marangon, C.A.; Amaro Martins, V.D.C.; de Guzzi Plepis, A.N. Chitosan/gelatin films with jatobá resin: Control of properties by vegetal resin inclusion and degree of acetylation modification. *Int. J. Biol. Macromol.* **2021**, *182*, 1737–1745.
29. Hui, B.; Zhang, Y.; Ye, L. Structure of PVA/gelatin hydrogel beads and adsorption mechanism for advanced Pb(II) removal. *J. Ind. Eng. Chem.* **2015**, *21*, 868–876. [[CrossRef](#)]
30. Maciejewski, H.; Marciniak, B.; Kownacki, I. Sposób Modyfikacji Polisiłoksanów PL 193 689 B1, 18 December 2000.
31. Marciniak, B.; Chadyniak, D.; Pawluć, P.; Maciejewski, H.; Błażejewska-Chadyniak, P. Sposób Otrzymywania Poli(Metylo,Alkilo) Siloksanów PL 194 668, 10 July 2006.
32. Fiedorow, R.; Dutkiewicz, M.; Marciniak, B.; Guliński, J.; Maciejewski, H. Sposób Otrzymywania Modyfikowanych (Poli)Siloksanów. PL 198290, 30 June 2008.
33. González-Paz, R.J.; Lligadas, G.; Ronda, J.C.; Galià, M.; Ferreira, A.M.; Boccafocchi, F.; Ciardelli, G.; Cádiz, V. Study on the interaction between gelatin and polyurethanes derived from fatty acids. *J. Biomed. Mater. Res. Part A* **2013**, *101A*, 1036–1046. [[CrossRef](#)] [[PubMed](#)]
34. Zhang, N.; Qiu, H.; Si, Y.; Wang, W.; Gao, J. Fabrication of highly porous biodegradable monoliths strengthened by graphene oxide and their adsorption of metal ions. *Carbon* **2011**, *49*, 827–837. [[CrossRef](#)]
35. Dwivedi, P.; Sahu, J.N.; Mohanty, C.R.; Mohana, B.R.; Meikap, B.C. Column performance of granular activated carbon packed bed for Pb(II) removal. *J. Hazard. Mater.* **2008**, *156*, 596–603. [[CrossRef](#)]
36. Kalak, T.; Kłopotek, A.; Cierpiszewski, R. Effective adsorption of lead ions using fly ash obtained in the novel circulating fluidized bed combustion technology. *Microchem. J.* **2019**, *145*, 1011–1025.
37. Lee, Y.C.; Chang, S.-P. The biosorption of heavy metals from aqueous solution by Spirogyra and Cladophora filamentous macroalgae. *Bioresour. Technol.* **2011**, *102*, 5297–5304. [[CrossRef](#)] [[PubMed](#)]
38. Laus, R.; Costa, T.G.; Szpoganicz, B.; Fávere, V.T. Adsorption and desorption of Cu(II), Cd(II) and Pb(II) ions using chitosan crosslinked with epichlorohydrin-triphosphate as the adsorbent. *J. Hazard. Mater.* **2010**, *183*, 233–241. [[CrossRef](#)] [[PubMed](#)]
39. Li, L.; Wang, Z.; Ma, P.; Bai, H.; Dong, W.; Chen, M. Preparation of polyvinyl alcohol/chitosan hydrogel compounded with graphene oxide to enhance the adsorption properties for Cu(II) in aqueous solution. *J. Polym. Res.* **2015**, *22*, 1–10. [[CrossRef](#)]
40. Li, G.; Wang, B.; Sun, Q.; Xu, W.Q.; Han, Y. Adsorption of lead ion on amino-functionalized fly-ash-based SBA-15 mesoporous molecular sieves prepared via two-step hydrothermal method. *Micropor. Mesopor. Mater.* **2017**, *252*, 105–115. [[CrossRef](#)]
41. Calero, M.; Hernainz, F.; Blázquez, G.; Martín-Lara, M.A.; Tenorio, G. Biosorption kinetics of Cd(II), Cr(III) and Pb(II) in aqueous solutions by olive stone. *Braz. J. Chem. Eng.* **2009**, *26*, 265–273. [[CrossRef](#)]
42. Kumar, P.S.; Gayathri, R. Adsorption of Pb<sup>2+</sup> ions from aqueous solutions onto bael tree leaf powder: Isotherms, kinetics and thermodynamics study. *J. Eng. Sci. Technol.* **2009**, *4*, 381–399.
43. El-Ashtoukhy, E.-S.Z.; Amin, N.K.; Abdelwahab, O. Removal of Lead(II) and Copper(II) from Aqueous Solution Using Pomegranate Peel as a New Adsorbent. *Desal* **2008**, *223*, 162–173. [[CrossRef](#)]
44. Blázquez, G.; Martín-Lara, M.A.; Dionisio-Ruiz, E.; Tenorio, G.; Calero, M. Evaluation and comparison of the biosorption process of copper ions onto olive stone and pine bark. *J. Ind. Eng. Chem.* **2011**, *17*, 824–833. [[CrossRef](#)]
45. Łużny, R.; Ignasiak, M.; Walendziewski, J.; Stolarski, M. Heavy metal ions removal from aqueous solutions using carbon aerogels and xerogels. *Chemik* **2014**, *68*, 544–553.
46. Magossi, M.S.; Maraldi, V.A.; Magossi, M.S.; Da Costa, F.M.; Alves, K.; Franco, F.D.S.; Do Carmo, D.R. A New Triazole-Thiol Compound Organofunctionalized on the Silica Gel Surface: Chemical Properties and Copper Sorption in Ethanol/Water Media. *Silicon* **2021**, *13*, 2243–2255. [[CrossRef](#)]
47. Ianași, C.; Picioruș, M.; Nicola, R.; Ciopec, M.; Negrea, A.; Nižňanský, D.; Len, A.; Almásy, L.; Putz, A.M. Removal of cadmium from aqueous solutions using inorganic porous nanocomposites. *Korean J. Chem. Eng.* **2019**, *36*, 688–700. [[CrossRef](#)]
48. Nicola, R.; Costișor, O.; Ciopec, M.; Negrea, A.; Lazău, R.; Ianași, C.; Picioruș, E.-M.; Len, A.; Almásy, L.; Szerb, E.I.; et al. Silica-Coated Magnetic Nanocomposites for Pb<sup>2+</sup> Removal from Aqueous Solution. *Appl. Sci.* **2020**, *10*, 2726. [[CrossRef](#)]
49. Mishra, S.P. Adsorption–desorption of heavy metal ions. *Curr. Sci.* **2014**, *107*, 601–612.